Smart Structures and Systems, *Vol. 14, No. 2 (2014) 71-83*
DOI: http://dx.doi.org/10.12989/sss.2014.14.2.71

Effects of photostrictive actuator and active control of flexible membrane structure

S.C. Gajbhiye[1a], S.H. Upadhyay[*2] and S.P. Harsha[2b]

[1]*Vishwavidyalaya Engineering College, Saguja Univeristy, Ambikapur, Chhattisgarh-497001, India*
[2]*Indian Institute of Technology Roorkee, Uttarakhand-247667, India*

(Received October 19, 2012, Revised June 23, 2013, Accepted June 23, 2013)

Abstract. The purpose of this paper is to investigate the flexible structure of parabolic shell using photostrictive actuators. The analysis is made to know its dynamic behavior and light-induced control forces for coupled parabolic shell. The effects of an actuator location as well as membrane and bending components under the control action have been analyzed considering the approximate spherical model. The parabolic membrane shell accuracy is being mathematically approximated and validated comparing the light induced control forces using approximate equivalent spherical shell model. The parabolic shell with kapton smart material and photostrictive actuators has been used to formulate the governing equation in the transverse direction. The Kirchhoff-Love assumptions are used to obtain the governing equation of shell with actuator. The mechanical membrane forces and bending moments for parabolic thin shell with actuator is used to analyze the dynamic effect. The results show that membrane control action is much more significant than bending control action. Photostrictive actuators oriented along circumferential direction (actuator-2) can give better control effect than actuators placed along longitudinal direction (actuator-1). The slight difference is observed between spherical and parabolic shell for a surface with focal length to the diameter ratio of 1.00 or more than unity. Space applications often have the shape of parabolical shells or shell of revolution, due to their required focusing, aiming, or reflecting performance. The present approach is focused that photostrictive actuators can effectively control the vibration of parabolical membrane shell. Also, the actuator's location plays an important role in defining the control force.

Keywords: parabolic shells; spherical shell; actuators; membrane effect; bending effect

1. Introduction

Over the last few decades, studying the dynamic behaviors of an inflatable membrane structure has proven to be a challenging job. Many researchers have been studied the dynamic characterization of membranes (Gajbhiye *et al.* 2012, Jenkins 1996, Jha *et al.* 2002, Saigal *et al.,* 1986) using numerical methods such the pre-stress effects on the membrane, wrinkling effects due to pressure loading, surface deviations, and when possible, experimental approaches (Leyland *et al.* 2005, Jenkins and Korde 2006) to compute vibration modes and frequencies of an inflatable

∗Corresponding author, Professor, E-mail: upadhyaysanjayh@yahoo.com
[a] Assistant Professor, E-mail: scg.gajbhiye@gmail.com
[b] Professor, E-mail: spharsha@gmail.com

http://www.techno-press.org/?journal=sss&subpage=8 ISSN: 1738-1584 (Print), 1738-1991 (Online)

structures. This research is not now limited to the mode shape analysis and frequency analysis. The various parameters like active control using actuators and sensor (Shih 2000) play a major role in optimizing the shape and size. This optimization leads the shape of membrane structure in the required focusing, aiming, or reflecting performance. The parabolic curvature shell of revolution (Fig. 1) is one of the most difficult geometries among all shell and non-shell structures. Extensive studies have been carried out to achieve active control of high-performing flexible structures called 'smart structures' (Lim *et al.* 1999, Crawley 1994) with the help of piezoelectric materials (Tzou 1998), shape-memory alloys (Ma *et al.* 2004), etc. Since these smart material sensor/actuator systems are either surface-bounded or embedded in structures, hard-wired connections. However, these are required to transmit control commands. In many operating environments, the metallic signal wires are likely to attract electrical noise that will contaminate the control signals. To remedy this situation, optically driven and remotely actuated photostrictive actuators have been proposed (Uchino *et al.* 2001, Liu and Tzou 1998, Uchino 1990, 1996, Fukuda *et al.* 1993). The principal advantages of photostrictive actuators, can directly convert photonic energy to mechanical motion and pulses of light instead of electric voltages. Neither needs electric lead wires nor electric circuits as hard-wire connections may not be feasible or desirable in hostile environments and applications. Photostrictive behavior can be described as a superposition of a bulk photovoltaic effect and converse piezoelectric effect, these both induce mechanical strain. The analytical models of a beam with photostrictive actuators (Shih *et al.* 2005a) have been derived; likewise, PLZT (Lanthanum-modified lead zirconate titanate) ceramic has been researched widely because of its easy fabrication and relatively high photostriction (Sun and Tong 2007, 2008), PLZT bimorph was also used in an optical servo system by (Liang *et al.* 2006). The dynamics analysis of a two-Link flexible arm using a hybrid variable structure (Mirzaee *et al.* 2010) and a single flexible arm with the PZT patches as a sensor and actuator has been work out using extended Hamilton method; this research reflected the control trajectory and active vibration suppression of a single-link flexible arm using piezoelectric materials (Mirzaee *et al.* 2011).

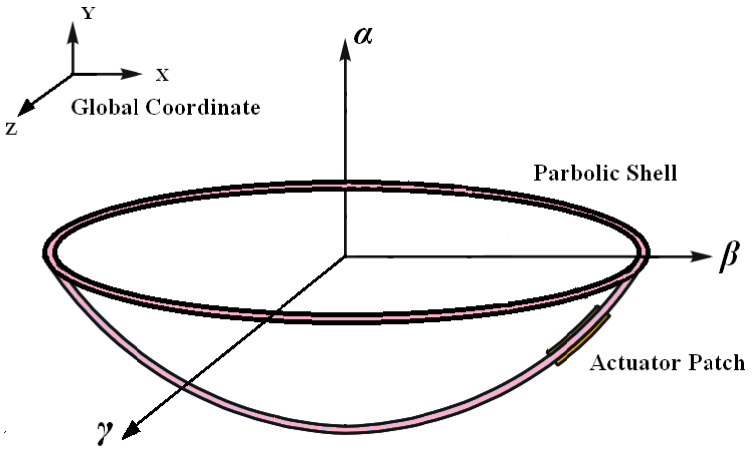

Fig. 1 Parabolidal shell with actuators patch

The applications of photostrictive actuators for shape and displacement control have been evaluated in (Guo *et al.* 2007, Wang *et al.* 2009). (Shih *et al.* 2006, 2007), also investigated the photonic control of shallow spherical and parabolic using the photostrictive actuators. However, the signal analysis of photostrictive laminated membrane shell with free boundary condition has been further investigated (Yue 2007). Furthermore, the uses of optoelectromechanical photostrictive materials for structronics system have been found in of references (Tzou *et al.* 1996, Shih *et al.* 2005b). Since, the photostrictive actuator system has neither electric lead wires nor electric circuits, so it is relatively immune to electro-magnetic interference. Due to the relatively high piezo-electric coefficient and ease of fabrication, the photostrictive actuator is ideal for use in harsh environmental conditions with strong magnetic and electric disturbances. Photostrictive actuators can be driven only by the irradiation of light, hence suitable to use as actuators in which lead wires can hardly be connected because of their ultra-small size or of their employed conditions such as ultra-high vacuum or outer space. This paper presents an investigation towards the modeling and control of shells integrated with photostrictive actuators with governing equation and the solution procedure. The actuators controlling forces at various locations on parabolic and spherical shells are investigated. The various issues like actuators position, membrane and bending effects have been discussed. This may help in designing the mechanical system with photostrictive actuators for practical applications.

2. Parabolidal membrane shell accuracy with spherical approximation

The local curvature of a parabolidal surface varies with distance from the apex. The basic front view of the parabolic shell is shown in Fig. 2. The focal length to diameter ratio is *(F/D)* provides a measure of the depth or shallowness of the reflector cross section. The focal length calculation is done by

$$F = D^2 / 16M' \tag{1}$$

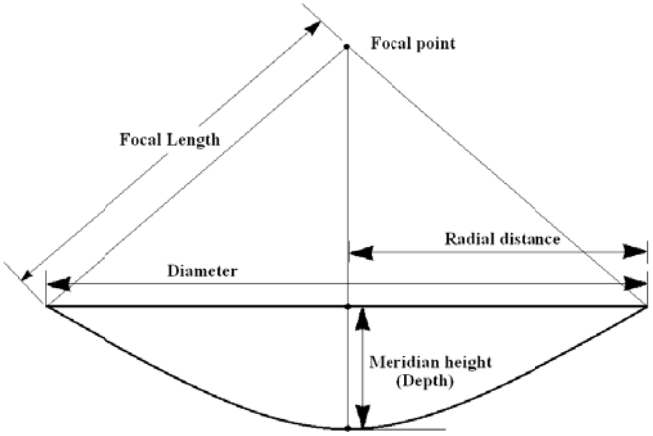

Fig. 2 Front view of the parabolic shell

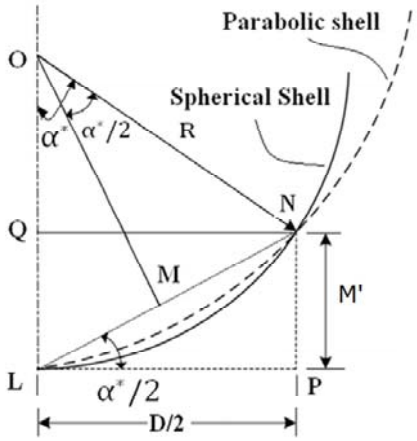

Fig. 3 Spherical approximation to the parabolic shell

It is found to be truth that the curvature of a parabola deviates by less than 1% from the equivalent spherical shape once the radius of the aperture has not exceeded 20% of the radius of the curvature (Glaese 2003). In other words, the difference between a spherical shell and a parabola is under 1% for surface with a focal length to the diameter ratio *(F/D)* of one more than unity. This can be critical for optical purposes but not believed to be a source of significant change in dynamic behavior. Therefore, to govern the simplicity of the dynamic performance of the parabolic shell, an equivalent spherical shell is considered in which the spherical shell of radius R coincides with parabolic surface both at the apex and at the edge (Tan and Pellegrino 2004), as shown in Fig. 3.

For a parabolic shell, from ΔLPN

$$\sin\frac{\alpha^*}{2} = \frac{M'}{\sqrt{\left(\left(\frac{D}{2}\right)^2 + M'^2\right)}} \tag{2}$$

From ΔOMN,

$$\sin\frac{\alpha^*}{2} = \frac{\sqrt{\left(\left(\frac{D}{2}\right)^2 + M'^2\right)}}{2R} \tag{3}$$

Since the both Δ's are equal, therefore the spherical shell radius can be found as

$$R = 2F + \frac{D^2}{32F} \tag{4}$$

Now, from ΔOQN

$$\sin\alpha^* = \frac{D}{2R} \tag{5}$$

From Eqs. (3) and (4), the subtended angle α^* in terms of focal length can be found as

$$\alpha^* = \frac{D}{\left[4F + D^2/16F\right]} \tag{6}$$

3. Parabolidal membrane shell modeling with photostrictive actuators

In the fields of mechanical, architectural and aeronautical engineering, the parabolidal shells are mostly utilized to expose good dynamical behaviors and its focusing characteristics. The mathematical modeling of parabolidal shells with photostrictive is presented in this section. Parabolidal shells are fabricated as flexible and low damping components which need to be micro-controlled. Parabolic shells of revolution are common components for reflectors, mirrors, etc. Photostrictive materials produce mechanical strain when irradiated by ultraviolet light, thus can be used in wireless control of structures.

Under the domain of global coordinate system *(X,Y,Z)*, the parabolic shell is defined along the meridional, circumferential and transverse directions (Fig. 3), denoted respectively by *α, β* and *γ* for tri-orthogonal curvilinear coordinate system *(α,β,γ)*. The radial distance and meridian height at the pole respectively, be denoted by *R* and *M'*. The constant ң represented by $H' = 2R/M'$. The two principal radii of double curvature are $R_\alpha = \frac{\beta}{\cos^3\alpha}$ and $R_\beta = \frac{\beta}{\cos\alpha}$. Membrane approximation is applied for parabolidal membrane shells in which the rotary inertial effects and the transverse shear deformations are neglected in thin shells revolution. The lame's parameters can be defined as $A_i = R_\alpha$ and $A_j = \frac{\beta}{\cos\alpha}\sin\alpha$. The fundamental system equation of the parabolidal shell (Tzou 1993) can be written as

$$\frac{\partial(R_\beta N_{\alpha\alpha}\sin\alpha)}{\partial\alpha} + R_\alpha\frac{\partial N_{\beta\alpha}}{\partial\beta} - N_{\beta\beta}R_\alpha\cos\beta + R_\alpha R_\beta\sin\alpha\left(\frac{Q_{\alpha\gamma}}{R_\alpha} + F_X\right) = R_\alpha R_\beta\sin\alpha\rho h\frac{\partial^2 u_\alpha}{\partial t^2} \tag{7}$$

$$\frac{\partial(R_\beta N_{\alpha\beta}\sin\alpha)}{\partial\alpha} + R_\alpha\frac{\partial N_{\beta\beta}}{\partial\beta} - N_{\beta\alpha}R_\alpha\cos\beta + R_\alpha R_\beta\sin\alpha\left(\frac{Q_{\beta\gamma}}{R_\beta} + F_Y\right) = R_\alpha R_\beta\sin\alpha\rho h\frac{\partial^2 u_\beta}{\partial t^2} \tag{8}$$

$$\frac{\partial(R_\beta N_{\alpha\gamma}\sin\alpha)}{\partial\alpha} + R_\alpha\frac{\partial N_{\beta\gamma}}{\partial\beta} - R_\alpha R_\beta\sin\alpha\left(\frac{N_{\alpha\alpha}}{R_\alpha} + \frac{N_{\beta\beta}}{R_\beta}\right) + R_\alpha R_\beta\sin\alpha(F_Z) = R_\alpha R_\beta\sin\alpha\rho h\frac{\partial^2 u_\gamma}{\partial t^2} \tag{9}$$

where

$$Q_{\alpha\gamma} = \frac{1}{R_\alpha R_\beta\sin\alpha}\left[\frac{\partial(R_\beta M_{\alpha\alpha}\sin\alpha)}{\partial\alpha} + R_\alpha\frac{\partial M_{\beta\alpha}}{\partial\beta} - M_{\beta\beta}R_\alpha\cos\alpha\right] \tag{10}$$

$$Q_{\beta\gamma} = \frac{1}{R_\alpha R_\beta \sin\alpha}\left[\frac{\partial(R_\beta M_{\beta\alpha}\sin\alpha)}{\partial\alpha} + R_\alpha \frac{\partial M_{\beta\beta}}{\partial\beta} - M_{\beta\alpha}R_\alpha \cos\alpha\right] \tag{11}$$

Imposing the Kirchhoff-Love assumptions and neglecting the twisting in the plan effect of the shells, the some membrane and bending strains can be defined as follows

$$s^m{}_{\gamma\gamma} = s^m{}_{\alpha\gamma} = s^m{}_{\beta\gamma} = 0 \tag{12}$$

$$s^m{}_{\alpha\alpha} = \frac{\cos^3\alpha}{H'}\left(\frac{\partial u_\beta}{\partial\beta} + u_\gamma\right) \tag{13}$$

$$s^m{}_{\beta\beta} = \frac{\cos\alpha}{H'\sin\alpha}\left(\frac{\partial u_\beta}{\partial\beta} + u_\alpha\cos\alpha + u_\gamma\sin\alpha\right) \tag{14}$$

$$s^m{}_{\alpha\beta} = \frac{\cos\alpha}{H'\sin\alpha}\left(\frac{\partial u_\alpha}{\partial\beta} + \cos^2\alpha\sin\alpha\frac{\partial u_\beta}{\partial\alpha} - u_\beta\cos\alpha\right) \tag{15}$$

$$k^b{}_{\alpha\alpha} = \frac{\cos^6\alpha}{H'^2}\left(\frac{\partial u_\alpha}{\partial\alpha} - \frac{\partial^2 u_\gamma}{\partial\alpha^2}\right) - \frac{3\cos^5\alpha\sin\alpha}{H'^2}\left(u_\alpha - \frac{\partial u_\gamma}{\partial\alpha}\right) \tag{16}$$

$$k^b{}_{\beta\beta} = \frac{\cos^2\alpha}{H'^2\sin\alpha}\left(\frac{\partial u_\beta}{\partial\beta} - \frac{1}{\sin\alpha}\frac{\partial^2 u_\gamma}{\partial\beta^2} + \cos^3\alpha\left(u_\alpha - \frac{\partial u_\gamma}{\partial\alpha}\right)\right) \tag{17}$$

$$k^b{}_{\alpha\beta} = \frac{\cos^3\alpha}{H'^2\tan\alpha}\frac{\partial u_\alpha}{\partial\beta} - \frac{2\cos^3\alpha}{H'^2\tan\alpha}\frac{\partial u_\gamma}{\partial\beta\partial\alpha} + \frac{\cos^4\alpha}{H'^2}\frac{\partial u_\beta}{\partial\alpha} + \frac{2\cos\alpha}{H'^2\tan^2\alpha}\frac{\partial u_\gamma}{\partial\beta} - \left(\frac{2\cos^5\alpha + \cos^2 2\alpha}{2H'^2\sin\alpha}\right)u_\beta \tag{18}$$

Using the relations from Eqs. (12) to (18) as, the mechanical membrane forces and bending moments for thin shell can be followed as

$$N_{\alpha\alpha} = K^m\left(s^m{}_{\alpha\alpha} + \mu s^m{}_{\beta\beta}\right) \tag{19}$$

$$N_{\beta\beta} = K^m\left(s^m{}_{\beta\beta} + \mu s^m{}_{\alpha\alpha}\right) \tag{20}$$

$$N_{\alpha\beta} = N_{\beta\alpha} = \frac{K^m(1-\mu)}{2}s^m{}_{\alpha\beta} \tag{21}$$

$$M_{\alpha\alpha} = K^b\left(k^b{}_{\alpha\alpha} + \mu k^b{}_{\beta\beta}\right) \tag{22}$$

$$M_{\beta\beta} = K^b\left(k^b{}_{\beta\beta} + \mu k^b{}_{\alpha\alpha}\right) \tag{23}$$

$$M_{\alpha\beta} = M_{\beta\alpha} = \frac{K^b(1-\mu)}{2}k^b{}_{\alpha\beta} \tag{24}$$

Noting that $K^m = \dfrac{Eh}{(1-\mu^2)}$ and $K^b = K^m * \dfrac{h^2}{12}$; The different assumptions from flexible membrane approximation (Soedel 1981) have been followed to avoid the complication in the fundamental equation as thin parabolidal shell has non-constant double curvature. The system equations i.e., Eqs. (7)-(24) for the parabolidal shell shall be reduced to

$$\frac{\partial(N_{\alpha\alpha}\tan\alpha)}{\partial\alpha}+\frac{1}{\cos^3\alpha}\frac{\partial N_{\beta\alpha}}{\partial\beta}-\frac{N_{\beta\beta}}{\cos^2\alpha}=H'\frac{\sin\alpha}{\cos^4\alpha}\rho h\frac{\partial^2 u_\alpha}{\partial t^2} \tag{25}$$

$$\frac{\partial(N_{\alpha\beta}\tan\alpha)}{\partial\alpha}+\frac{1}{\cos^3\alpha}\frac{\partial N_{\beta\beta}}{\partial\beta}+\frac{N_{\beta\alpha}}{\cos^2\alpha}=H'\frac{\sin\alpha}{\cos^4\alpha}\rho h\frac{\partial^2 u_\beta}{\partial t^2} \tag{26}$$

$$-N_{\alpha\alpha}\tan\alpha-\frac{N_{\beta\beta}\sin\alpha}{\cos^3\alpha}=H'\frac{\sin\alpha}{\cos^4\alpha}\rho h\frac{\partial^2 u_\gamma}{\partial t^2} \tag{27}$$

In the dynamic analysis, the transverse oscillation of the paraboloidal shell dominates the entire system and hence controlled by the photostrictive actuators. The photostrictive actuators are introduced on both upper and lower surface of the parabolic structure to control the moments induced by the actuators. The actuators should be placed either along meridional or circumferential direction. If the actuator systems are supposed to provide control force $N_{\alpha\alpha}$ then the actuators should be placed in α-direction (actuator-1). If the system needs to control force $N_{\beta\beta}$, the photostrictive actuators should be oriented in β-direction (actuator-2).

The governing equation of the flexible parabolic membrane shell with actuator(s) in the transverse direction can be given as

$$\frac{\cos^3\alpha}{H'}N_{\alpha\alpha}+\frac{\cos\alpha}{H'}N_{\beta\beta}+\rho h\frac{\partial^2 u_\gamma}{\partial t^2}=\frac{\cos^3\alpha}{H'}N^1{}_{\alpha\alpha} \quad \text{(for } A\text{-}1\text{)} \tag{28}$$

$$\frac{\cos^3\alpha}{H'}N_{\alpha\alpha}+\frac{\cos\alpha}{H'}N_{\beta\beta}+\rho h\frac{\partial^2 u_\gamma}{\partial t^2}=\frac{\cos^3\alpha}{H'}N^2{}_{\beta\beta} \quad \text{(for } A\text{-}2\text{)} \tag{29}$$

where, the actuator's controlling force induced given by (Shih and Tzou 2007)

$$N^1{}_{\alpha\alpha}=h_a Y_a \bar{s}[u_s(\alpha-\alpha_1^*)-u_s(\alpha-\alpha_2^*)][u_s(\beta-\beta_1^*)-u_s(\beta-\beta_2^*)] \quad \text{(for } A\text{-}1\text{)} \tag{30}$$

$$N^2{}_{\beta\beta}=h_a Y_a \bar{s}[u_s(\alpha-\alpha_1^*)-u_s(\alpha-\alpha_2^*)][u_s(\beta-\beta_1^*)-u_s(\beta-\beta_2^*)] \quad \text{(for } A\text{-}2\text{)} \tag{31}$$

In the above expression, even though the nomenclature looks same, but the numeric value depends on the actuators properties and their shape and size. Since the transverse response is the combination of the multiple modes, using the model expansion method (Tzou 1993), the kth model equation of the parabolidal shell in the transverse direction can be obtained as

$$\frac{\partial^2\eta_k}{\partial t^2}+2\zeta_k\omega_k+\frac{\partial\eta_k}{\partial t}+(\omega_n)^2\eta_k=F_k^c \tag{32}$$

and the control force can be obtained as

$$F_k^c = \frac{A_k(k+1)h_a Y_a \bar{s} H'\left[\sin(k\beta_2^*) - \sin(k\beta_1^*)\right]}{\rho h N_k} \quad \text{(for } A\text{-}1\text{)} \tag{33}$$

$$F_k^c = \frac{A_k(k+1)h_a Y_a \bar{s} H'\left[\sin(k\beta_2^*) - \sin(k\beta_1^*)\right]}{\rho h N_k} \quad \text{(for } A\text{-}2\text{)} \tag{34}$$

where,

$$N_k = A_k^2 H'^2 (k+1)^2 \pi \int_0^{\alpha^*} \frac{\sin^{(2k+1)}\alpha}{\cos^2\alpha} d\alpha \tag{35}$$

where, α^* is meridional angle of boundary rim.

4. Control action of photostrictive actuator patches

The parabolidal shell can be actively controlled by the photostrictive actuators. The photostrictive actuators can be activated under high energy light illumination. The light intensity can be decided according to some control laws, called as control input. Since, light intensity is related to model velocity, and hence the *kth* model governing equation Eq. (31) of the parabolidal shell for the instant time *t* can be reframed as

$$\ddot{\eta}_{kj} + 2\zeta_k \omega_k + \dot{\eta}_{kj} + (\omega_n)^2 \eta_k = F_{kj}^c \tag{36}$$

Where, suffix *j* denotes for the time instant t_j and solved using Newmark-β method. In this paper, the constant light intensity control is used. The amplitude of light intensity is constant and can be determined (Wang 2011) as

$$I(t_j) = G_1[\max|\dot{\eta}_k t|] \tag{37}$$

It is assumed, when light direction get changed the remnants strain and electric field of an actuator, disappear immediately. Since, both the actuators are laminated with the parabolidal shell, light direction should be alternatively applied to the top and bottom of the photostrictive actuators depending on velocity direction. When the parabolidal shell oscillates downward, light should be applied to the bottom actuators so that positive control force can be induced; when the parabolidal shell oscillates upward then light should be applied to the top actuators, and negative control force can be induced.

5. Result and discussion

Since the placement of actuators, is one of the critical problems in structural active control, hence the effects of the actuator's location along the meridional and circumferential direction have been analyzed. The parabolic shell is taken which is made up of kapton smart material having young's modulus as 2.55×10^9 N/m^2, density as 1420 kg/m^3 and Poisson's ratio of 0.36. The geometric parameters are R = 0.1 m, M'= 0.1 m and $h = 1 \times 10^{-3}$ m. The shell is controlled by the photostrictive

actuators whose geometric parameters are of length $2x10^{-2}$ m, width 0.75 x 10^{-2} m and uniform thickness of $1x10^{-4}$ m, and the material properties of photostrictive actuators are listed in Table 1 (Shih 2005b).

Table 1 Material properties of photostrictive actuators

No.	Material properties	Value
1	Saturated electric field	$2.4x10^{5}$ V.m^{-1}
2	Young's modulus	$6.30x10^{10}$ N/m^{2}
3	Optical actuator constant	$2.772x10^{-3}$ m^{2}W^{-1}s^{-1}
4	Voltage leakage constant	0.01 Vs^{-1}
5	Power of absorbed heat	0.023 m^{2}s^{-1}
6	Piezoelectric strain constant	$1.79x10^{-10}$ mV^{-1}
7	Heat capacity	16 W^{o}C^{-1}
8	Heat transfer rate	0.915 W^{o}C^{-1}s^{-1}
9	Stress-temperature constant	6.808 $6x10^{4}$ N·m^{-2}C^{-1}
10	Pyroelectric constant	$0.25x10^{-4}$ C·m^{-2}C^{-1}
11	Electric permittivity	$1.65x10^{-8}$ Fm^{-1}

The two different orientations have been chosen for both actuators. The actuator-1 is placed along α-direction and its polarity also kept in the same direction. Similarly, the actuator-2 lies along β-direction with polarity in the same direction. In all four mode shape, the deflection of the edge due to model control action for free parabolic membrane shell is clearly observed corresponding to the actuator's orientation. From the set of figure 4, it is concluded that the control action of an induced force of actuator-2 is more than that of actuator-1. The control action induced by photostrictive actuator along meridional direction is larger than that of the actuator along the circumferential direction. It is so because the locations of actuators are closed and equally dense due to the light intensity towards the rim of the shell as compared to the location of actuator-2.

The Fig. 5 shows the bending and membrane effect corresponding to actuator-2's location at its mid-point where this actuator is located at the bottom of the rim of the spherical shell. In this figure, the first mode shows the variation of actuation force along the spherical shell surface in the meridional direction. This remarked that the membrane force dominates the overall control effects. Figs. 5 and 6 respectively, expose the same conclusion to that of the spherical shell and the parabolic shell with the actuator-2 at the bottom rim for the first mode shape.

The first four mode shapes have been shown in Fig. 6, indicating the comparison of the magnitude of actuator force induced by the intensity of light. As the actuator patch location moved away from the rim, the control forces may get decreased. This figure reveal that the control action increases from the pole to the boundary and the mode number increases as the actuation force decreases, this may conclude that the membrane effect gradually diminishes as the mode increases. The F/D ratio for the control induced force have been calculated and plotted for the three F/D ratio

of 0.50, 0.75, 1.00 and 1.25. as shown in Fig. 7. This figure shows good agreement for both models as the comparison of F/D ratio are equivalent. This may conclude that the difference between spherical shell and parabola shell become minimize with F/D of unity or more than unity.

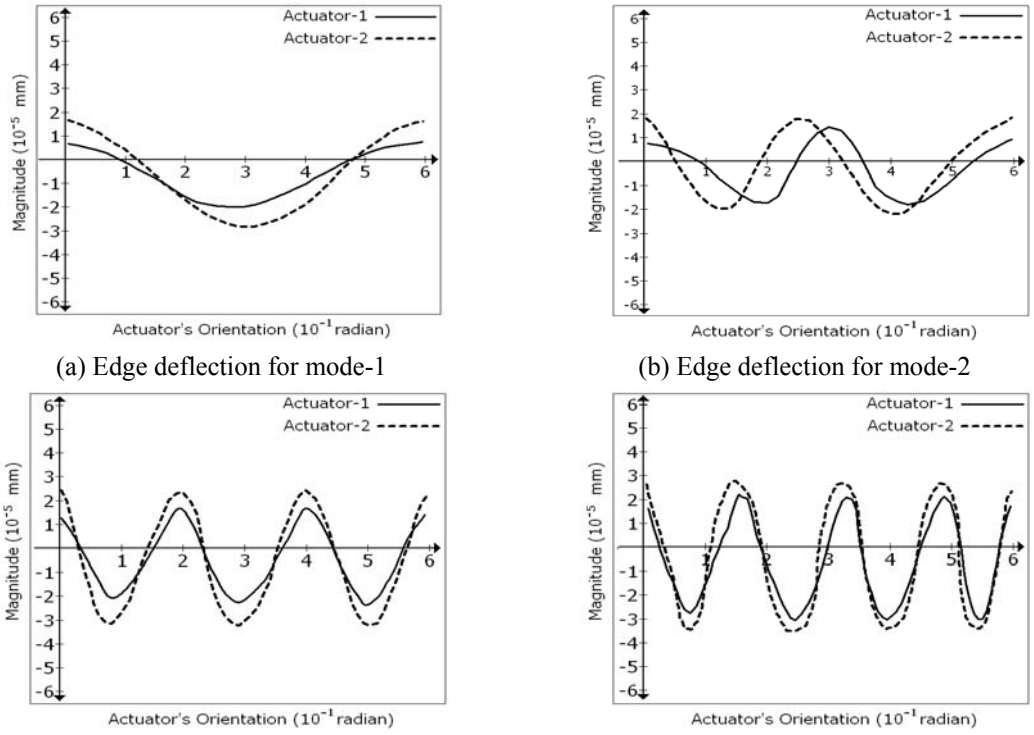

(a) Edge deflection for mode-1

(b) Edge deflection for mode-2

(c) Edge deflection for mode-3

(d) Edge deflection for mode-4

Fig. 4 Model control action of free parabolidal membrane shell with (a) edge deflection for mode-1, (b) edge deflection for mode-2, (c) edge deflection for mode-3, and (d) edge deflection for mode-4

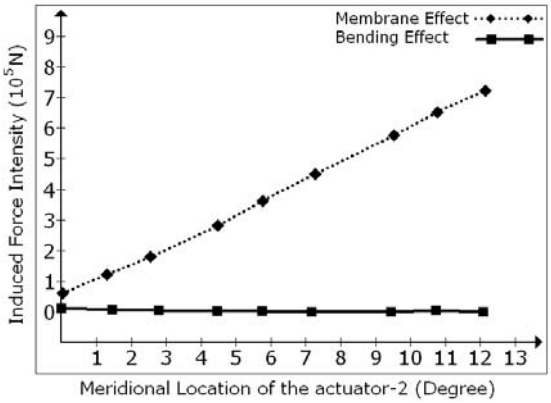

Fig. 5 Induced Force effect of actuator-2 at various positions for spherical shell showing membrane and bending effect for first mode shape

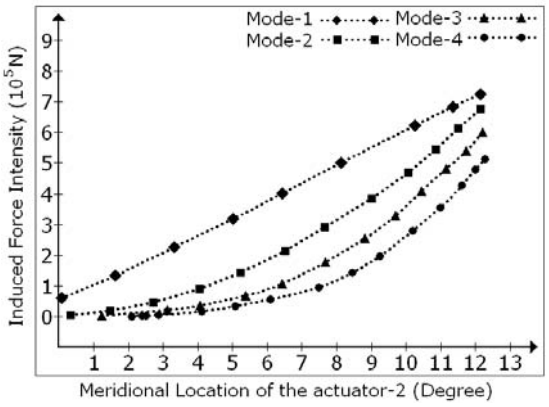

Fig. 6 Induced Force effect of acturator-2 at various positions for parabolic shell showing membrane effect for first four mode shape

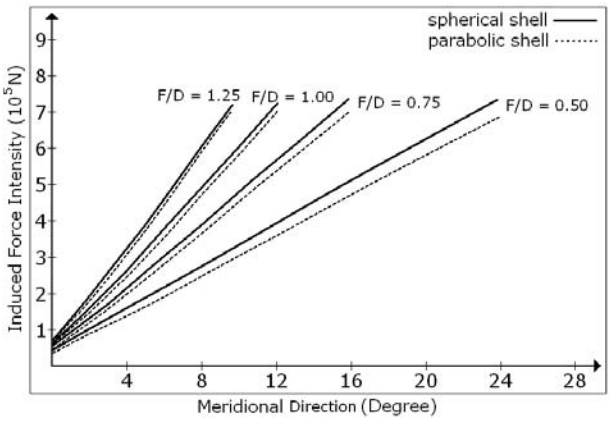

Fig. 7 Spherical and parabolic shell model comparison in terms of F/D

6. Conclusions

The dynamics behavior of the inflated parabolidal structure is of practical interest to spacecraft system and structural design as the parabolic shaped element is one of the key component of many inflated structure design due to their required focusing, aiming, or reflecting performance. In this work, mathematical modeling with actuator patch, dynamic characteristics and mode shape functions of flexible parabolidal membrane shells are presented. The actuation force with control effects and the actuator locations have been evaluated. The accuracy of the parabolic shell is done by using spherical approximation. The following observations are carried out:

a) The control action of an induced force of actuator-2 is more than that of actuator-1 i.e., the control action induced by photostrictive actuator along meridional direction is larger than that of the actuator along the circumferential direction.

b) Membrane effects dominate much more compare to that of the bending effect. As the actuator patch location moved away from the rim, the control forces may get decreased. This Fig. 6 reveals that the control action increases from the pole to the boundary and the model actuation force gradually decreases at higher modes; this may conclude that the membrane effect gradually diminishes as the mode increases.

c) A parabolic shell is very complicated to analyze due to its non-constant radius, hence the accuracy of approximating a parabolic shell is done using spherical shell prediction. Figs. 5 and 6, reveals the same results for the first mode in the membrane effect.

d) To analyze the flexible parabolic shell, the results of the equivalent spherical shell have been compared and optimize the parabolic shell results if the focal length with diameter ratio should be kept unity or more than unity.

References

Crawley, E.F. (1994), "Intelligent structures for aerospace - A technology overview and assessment", *AIAA J*., **32**(8), 1689-1699.

Fukuda, T., Hattori, S., Arai, F., Matsuura, H., Hiramatsu, T., Ikeda, Y. and Maekawa, A. (1993), "Characteristics of optical actuator – servo-mechanisms using bimorph optical piezoelectric actuator", *Proceedings of the Conf. on 1993 IEEE Robotics and Automation*.

Gajbhiye, S.C., Upadhyay, S.H. and Harsha, S.P. (2012), "Free vibration analysis of flat thin membrane", *J. Eng. Sci. Tech*., **4**(8), 3942-3948.

Glaese, R.M., Regelbrugge, M.E., Lore, K.F., Smith, S.W. and Flint, E.M. (2003), "Modeling the dynamics of large diameter doubly curved shells made from thin-films", *Proceedings of the 44th AIAA/ASME/ASCE/AHS Structures, Structural Dynamics, and Materials Conference*, AIAA-2003.

Guo, Y.L., Zhou, J., Huang, Y. and Bao, M.H. (2007), "Modeling of photo induced deformation in silicon micro cantilever", *J. Sensors*, **7**, 1713-1719.

Jenkins, C.H. (1996), "Non-linear dynamic response of membranes: state of the art-update", *J. Appl. Mech. Rev*., **49**(10), 41-48.

Jenkins, C.H. and Korde, U.A. (2006), "Membrane vibration experiments: An historical review and recent results", *J. Sound Vib*., **295**(3-5), 602-613.

Jha, A.K., Inman, D.J. and Plaut, R.H. (2002), "Free vibration analysis of an inflated toroidal shell", *J. Vib. Acoust*., **124**(3), 387-396.

Leyland, Y.G., Ramanathan, S., Jiazhu Hu, and Pai, P.F. (2005), "Numerical and experimental dynamic characteristics of thin-film membranes", *Int. J. Solids Struct*., **42**, 3001-3025.

Liang, L. Wang, S. and Cao, F. (2006), "Research on dynamic characteristic of optical drive servo system with PLZT", *Proceedings of the 6th International Symposium on Instrumentation and Control Technology*. Beijing, China.

Lim, Y.H, Gopinathan, S.V., Varadan, V.V. and Varadan, V.K. (1999), "Finite element simulation of smart structures using an optimal output feedback controller for vibration and noise control", *Smart Mater. Struct.*, **8**(3), 324-337.

Liu, B. and Tzou, H.S. (1998), "Distributed photostrictive actuation and opto-piezo thermoelasticity applied to vibration control of plates", *J. Vib. Acoust*., **120**(4), 937-943.

Ma, N., Song, G. and Lee, H.J. (2004), "Position control of shape memory alloy actuators with internal electrical resistance feedback using neural networks", *Smart Mater. Struct.*, **13**(4), 777-783.

Mirzaee, E., Eghtesad, M. and Fazelzadeh, S.A. (2010), "Maneuver control and active vibration suppression of a two-link flexible arm using a hybrid variable structure/lyapunov control design", *Acta Astronautica*, **67**(9-10), 1218-1232.

Mirzaee, E., Eghtesad, M. and Fazelzadeh, S.A. (2011), "Trajectory tracking and active vibration

suppression of a smart Single-Link flexible arm using a composite control design", *Smart Struct. Syst*., **7**(2), 103-116.
Saigal, S., Yang, T.Y., Kim, H.W. and Soedel, W. (1986), "Free vibration of a tire as a toroidal membrane", *J. Sound Vib*., **107**(1), 71-82.
Shih, H.R. (2000), "Distributed vibration sensing and control of a piezoelectric laminated curved beam", *Smart Mater. Struct.*, **9**(6), 761-766.
Shih, H.R. and Tzou, H.S. (2006), "Wireless control of parabolic shells using photostrictive actuators", *Proceedings of the IMECE'2006*. Chicago, USA.
Shih, H.R. and Tzou, H.S. (2007), "Photostrictive actuators for photonic control of shallow spherical shells", *Smart Mater. Struct.*, **16**(5), 1712-1717.
Shih, H.R., Watkins, J. and Tzou, H.S. (2005a), "Displacement control of a beam using photostrictive optical actuators", *J. Intell. Mat. Syst. Str*., **16**(4), 355-363.
Shih, H.R., Tzou, H.S. and Saypuri, M. (2005b), "Structural vibration control using spatially configured opto-electromechanical actuators", *J. Sound Vib.*, **284**(1-2), 361-378.
Soedel, W. (1981), *Vibrations of shell and plates*, Material Dekker Inc., New York.
Sun, D. and Tong, L. (2007), "Modeling of wireless remote shape control for beams using nonlinear photostrictive actuators", *Int. J. Solids Struct.*, **44**, 672-684.
Sun, D. and Tong, L. (2008), "Theoretical investigation on wireless vibration control of thin beams using photostrictive actuators", *J. Sound Vib.*, **312**(1-2), 182-194.
Tan, L.T. and Pellegrino, S. (2004), *Ultra thin deployable reflector antennas*, *AIAA, Paper 2004,* 1730.
Tzou, H.S. (1993), *Piezoelectric shells (distributed sensing and control of continua)*, Kluwer Academic Publishers, Boston, Dordrecht.
Tzou, H.S. (1998), "Multifield transducers,devices, mechatronic systems, and structronic systems with smart materials", *Shock Vib. Dig.*, **30**(4), 282-294.
Tzou, H.S. and Chou, C.S. (1996), "Non-linear opto-electro mechanics and photo deformation of optical actuators", *Smart Mater. Struct.*, **5**(2), 230-235.
Uchino, K. (1990), "Photostrictive actuators", *Proceedings of the IEEE 1990 Ultrasonic's Symp.*
Uchino, K. (1996), "New Applications of Photostriction", *Innovations Mater. Res*., **1**(1), 11-22.
Uchino, K., Poosanaas, P. and Tonooka, K. (2001), "Photostrictive actuators – new perspective", *Ferroelectrics*, **264**, 303-308.
Wang X., Yue H., Deng Z. (2011), "Active control of free paraboloidal membrane shells using photostrictive actuators", *Trans. Tianjin Univ*., **17**, 6-12.
Wang, X., Yue, H., Tzou, H.S. and Zonguan, D. (2009), "Actuation characteristics and control of thin cylindrical shells laminated with photostrictive actuators", *J. Vib. Shock*, **28**(9), 9-14.
Yue, H.H., Deng, Z.Q. and Tzou, H.S. (2007), "Distributed signal analysis of free-floating paraboloidal membrane shells", *J. Sound Vib*., **304**(3-5), 625-639.

CC